Biocatalysis and Agricultural Biotechnology 58 (2024) 103152

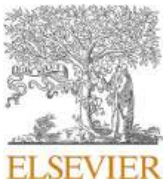

Contents lists available at ScienceDirect

Biocatalysis and Agricultural Biotechnology

journal homepage: www.elsevier.com/locate/bab

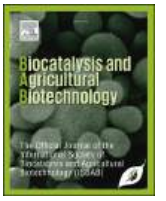

Investigation of α-glucosidase and α-amylase inhibition for antidiabetic potential of agarwood (*Aquilaria malaccensis*) leaves extract

Syahputra Wibowo [b], Sunia Kusuma Wardhani [a], Lisna Hidayati [a], Nastiti Wijayanti [a], Koichi Matsuo [c], Jessica Costa [d], Yudhi Nugraha [b], Josephine Elizabeth Siregar [b], Tri Rini Nuringtyas [a,e,*]

[a] *Faculty of Biology, Universitas Gadjah Mada, Jalan Teknika Selatan, Sekip Utara, Yogyakarta, 55281, Indonesia*
[b] *Eijkman Research Center for Molecular Biology, National Research and Innovation Agency (BRIN), Cibinong, Bogor, 16911, Indonesia*
[c] *Hiroshima Synchrotron Radiation Center, Hiroshima University, Higashi-Hiroshima, 739-0046, Japan*
[d] *Department of Biotechnology, Chemistry and Pharmacy, Università degli studi di Siena, Via A. Moro 2, 53100, Siena, Italy*
[e] *Research Center for Biotechnology, Universitas Gadjah Mada, Jalan Sekip Utara Yogyakarta, 55281, Indonesia*

ARTICLE INFO

Handling editor: Dr. Ching Hou

Keywords:
α-amylase
α-glucosidase
Antidiabetic
Aquilaria malaccensis Lamk
Molecular analysis

ABSTRACT

Diabetes mellitus is a metabolic disorder characterized by high blood sugar. The most common treatment is taking oral hypoglycemic drugs such as acarbose, but long-term use of acarbose has dangerous side effects. Thus, alternative therapies using herbal medicines are of interest to researchers. *Aquilaria malaccensis* leaves have been used as an herbal tea for their high antioxidant and antimicrobial activity. This research aimed to analyze the antidiabetic potential of *A. malaccensis* leaves extract in vitro and in silico. The research utilized a methodology that included the analysis of the inhibitory activity of α-amylase and α-glucosidase enzymes through spectrophotometry. Furthermore, the study examined the inhibition of glucose diffusion in the dialysis bag. Additionally, an in silico investigation on α-glucosidase inhibition was conducted, involving toxicity analysis of selected compounds, molecular docking, molecular dynamic simulation, and density functional theory. The results showed that chloroform extract of *A. malaccensis* leaves had the best result on each test parameter with an IC_{50} of 3.22 mg/mL for α-amylase inhibition and 3.65 mg/mL for α-glucosidase inhibition. The chloroform extract of *A. malaccensis* leaves is the best for inhibiting glucose diffusion in the first 30 min. All in silico models supported by density functional theory showed that some secondary metabolites of *A. malaccensis* leaves extract, such as 5-Hydroxy-4′,7-dimethoxyflavone and followed by epifriedelanol, are better than acarbose in terms of inhibiting α-glucosidase. Based on the results, agarwood's extract demonstrates anti-diabetic potential through the inhibition of α-amylase and exhibits a slightly superior efficacy in inhibiting α-glucosidase activity. This observation is substantiated by both in-laboratory and in-silico data.

* Corresponding author. Faculty of Biology, Universitas Gadjah Mada, Jalan, Teknika Selatan, Sekip Utara, Yogyakarta, 55281, Indonesia
E-mail addresses: putrawbw@gmail.com, syahputra.wibowo@brin.go.id (S. Wibowo), suniaksmw@gmail.com (S.K. Wardhani), lisna.hidayati@ugm.ac.id (L. Hidayati), nastiti_wijayanti@ugm.ac.id (N. Wijayanti), pika@hiroshima-u.ac.jp (K. Matsuo), jessica.costa2@unisi.it (J. Costa), yudhi.nugraha@brin.go.id (Y. Nugraha), jose001@brin.go.id (J.E. Siregar), tririni@ugm.ac.id (T.R. Nuringtyas).

https://doi.org/10.1016/j.bcab.2024.103152
Received 6 October 2023; Received in revised form 26 December 2023; Accepted 3 April 2024
Available online 19 April 2024

1. Introduction

High blood sugar levels are a hallmark of diabetes mellitus (DM), a metabolic condition caused by improper glucose absorption in the body. Impairment in carbohydrates, fats, and proteins metabolism is directly associated with this disease. (Archer et al., 2013). There are two types of diabetes mellitus, i.e., type 1 and type 2. The most prevalent type of diabetes is type 2, brought on by either a reduction in pancreatic insulin production or a decrease in the insulin receptor's sensitivity (Yeo et al., 2011). In the year 2021, the global prevalence of diabetes was documented at 537 million individuals, and an overwhelming majority, exceeding 90%, comprised cases of type 2 diabetes mellitus (T2DM). Among the top 10 countries with the highest rates of diabetes in adults, Asia asserted its prominence by securing six positions. Noteworthy nations in this ranking included China (with 140.9 million cases), India (reporting 74.2 million cases), and Pakistan (documenting 33 million cases) as the leading three countries, respectively (Venggadasamy et al., 2021). Diabetes mellitus is a progressive ailment impacting 10 million individuals in Indonesia, positioning the country as the fourth highest globally in terms of the prevalence of substantial diabetes cases, following India, China, and the United States. Projections indicate that by 2030, the number of DM cases in Indonesia is anticipated to escalate from 7 to 12 million (Nabila et al., 2022).

Once diagnosed with DM, a patient must live with the condition for the rest of his or her life. Consequently, changing one's lifestyle, especially diet, is frequently required for the efficient management of DM patients. This condition should be concomitant with pharmacotherapy, in which one needs a continuous consumption of oral chemical drugs to control the blood glucose level. Regular use of these medications lowers hepatic glucose production, reduces intestinal glucose absorption, and enhances insulin sensitivity (Chan et al., 2008). Patients who have severe conditions receive insulin injection therapy. However, the dose must be raised since prolonged medication usage leads to resistance and decreased insulin receptor sensitivity. Additionally, most Indonesians still find insulin treatments pricey (Herman and Kuo, 2021).

Another non-insulin-dependent treatment is an oral medicine containing digestive enzyme inhibitors such as α-amylase and α-glucosidase inhibitors. These inhibitors can decrease the intestinal absorption of glucose. Therefore, acarbose is the most often prescribed medication for this condition. However, after using acarbose for a long time, patients frequently have undesirable side effects, including diarrhea, gastrointestinal problems, flatulence, stomach discomfort, nausea, and headaches (Sudha et al., 2011). Besides that notably, there have been documented associations between the administration of α-glucosidase inhibitors, like acarbose, and the emergence of pneumatosis cystoides intestinalis (PCI) in individuals with DM, underscoring the potential side effects of such medication. Pneumatosis cystoides intestinalis is an uncommon gastrointestinal condition marked by the occurrence of numerous gas-filled cysts in the submucosa and/or subserosa of the intestinal wall, often accompanied by surrounding inflammation and fibrosis (McKinley et al., 2022).

The usage of herbal medicine has gained popularity recently around the world. Due to its historical reputation and the components derived from locally available natural resources, herbal medications are considered safer and more readily accessible. As a result, especially in rural regions, herbal medicines are considerably less expensive (Brusotti et al., 2014). The study on the activity of extract herbal on α-amylase and α-glucosidase inhibitor screening in medicinal plants has received much attention (Telagari and Hullatti, 2015; Joo et al., 2006).

Aquilaria malaccensis is one of Southeast Asia's most essential agarwood plants. The interaction between this plant and the microbes produces high-quality resin, making this plant the most cultivated among other agarwood plants. The distribution is widespread in Southeast and South Asia, including Indonesia, Myanmar, Malaysia, Singapore, and Bhutan (Hendra et al., 2016). Agarwood plants can be infected with microorganisms after three years of cultivation. Thus, while waiting for this optimal age, agarwood leaves can be used for herbal tea (Nuringtyas et al., 2018). The leaves of *A. malaccensis* were reported to have a high antioxidant and antimicrobial activity (Hendra et al., 2016) and protective effects on sperm quality of male rats and an aphrodisiac (Razak et al., 2019). As part of traditional medicines' ingredients, the leaves of *A. malaccensis* are believed to be very effective in treating inflammation, including diseases such as arthritis, asthma, and gout (Adam et al., 2017). Hence, the folk remedy acknowledges the leaves as an antipyretic, analgesic, and antidiabetic. Thus far, research involving *A. malaccensis* leaves in the context of diabetes mellitus has centered on active fractions that notably enhance glucose uptake in the skeletal muscle tissue of diabetic Wistar rats. This observation suggests potential therapeutic applications for diabetes. However, there is currently a gap in the literature concerning the pathway inhibition of proteins that play a role in the breakdown of carbohydrates into glucose. In this current research, we aimed to study the potency of the ethanol and chloroform extracts of *A. malaccensis* leaves as antidiabetic in vitro through their activity to inhibit α-amylase (EC 3.2.1.1) and α-glucosidase (EC 3.2.1.20) enzymes. The glucose diffusion assay was conducted to assess extract interactions with glucose. The metabolite content of the most potent extract from *A. malaccensis* leaves was analyzed, and major compounds were subjected to in silico analyses, including toxicity assessment and molecular docking for potential antidiabetic properties. Molecular dynamics simulations, followed by Principal Component Analysis (PCA), were employed to analyze the docking results. Compounds showing favorable binding affinity at the enzyme's catalytic site underwent further investigation using density functional theory in computational chemistry.

2. Results and discussion

2.1. Aquilaria malaccensis leaves extract

The extraction result using two different polarity solvents showed that the *A. malaccensis* leaves contained different amounts of nonpolar and polar metabolites. The final amount of ethanol extract mass was three times more than the chloroform extract, with 1.07 g and 0.37 g, respectively. The ethanol extract resulted in a thick paste with a dark green color with an oily look, while the chloroform extract was green and dry in color. Millaty et al. (2020) reported that the GC-MS profiles of extracts derived from chloroform were

dominated by fatty acids and fatty alcohols, while fatty acids dominated the ethanol extracts. On the other hand, Eissa et al. (2022) reported the presence of flavonoids in the ethanol extract. The ethanol extract was sequentially treated with n-hexane, dichloromethane, ethyl ethanoate, and n-butanol to obtain the corresponding extracts.

2.2. Inhibitory activity of Aquilaria malaccensis leaves extract on α-amylase and α-glucosidase

The α-amylase inhibition assay revealed that the ethanol extract had a lower inhibition activity to α-amylase enzyme than the chloroform extract, with an IC_{50} value of 14.75 mg/mL and 3.22 mg/mL, respectively. Similar trend was also observed on the α-glucosidase inhibition assay which showed the higher inhibition on chloroform extract over the ethanol extract with IC_{50} value of 3.65 ± 0.40 mg/mL and 6.64 ± 0.33 mg/mL, respectively. The chloroform extract of *A. malaccensis* leaves showed comparable inhibition activity with acarbose for both enzymes inhibition activities (Fig. 1.), α-amylase plays a key role in breaking down complex carbohydrates into simpler sugars, while α-glucosidase is involved in the final stages of carbohydrate digestion, converting disaccharides into glucose. The inhibition of these enzymes can effectively decelerate the absorption of glucose from the digestive tract, leading to a reduction in postprandial (after-meal) blood sugar spikes (Tundis et al., 2010).

Previous research indicates that a concentration of 10 mg/ml of acarbose demonstrated inhibitory effects of 68% and 70% on the activities of α-amylase and α-glucosidase, respectively. These results imply that the inhibitory impact of acarbose on both α-amylase and α-glucosidase is dependent on its concentration (Poovitha and Parani, 2016). This result indicating that the chloroform extract of *A. malaccensis* leaves has a high potency to inhibit the activity of carbohydrate-related digestive enzymes and may be chosen for further study as an alternative herbal medicine. Other studies also indicate congruent data that *A. malaccensis* leaves extract indeed demonstrates inhibitory capabilities against α-glucosidase, irrespective of the different extraction solvents used (Mat Rashid et al., 2020). Examining the data, it is evident that at the same concentration, acarbose exhibits slightly superior inhibition of α-glucosidase compared to its inhibition of α-amylase. This outcome aligns with the findings of this study, where the *A. malaccensis* extract also outperforms in inhibiting α-glucosidase. Consequently, for the in silico analysis, we have opted to proceed with the analysis specifically focusing on the α-glucosidase enzyme.

2.3. Assay of glucose diffusion inhibition

The capacity of secondary metabolites to bind glucose and lower free glucose in circulation may also contribute to maintaining blood glucose levels. Glucose diffusion assays were used to assess this capacity. The result showed that both ethanol and chloroform extracts showed effective glucose-binding properties. Compared to the distilled water which serves as the negative control, the ethanol and chloroform extracts showed a significant ability to reduce glucose diffusion to the outside dialysis bags, although the glucose concentration in both extracts increased with the longer observation time. Interestingly, Acarbose showed no inhibitory effects on the glucose movement to the external solution indicated by no significant different with the negative control (Fig. 2.).

These results may suggest that the ethanol and chloroform extracts can contribute to preventing postprandial hyperglycemia and have the potential to be used as antidiabetic drugs (Buthkar et al., 2018). Acarbose is classified as an oral antidiabetic drug whose action mechanism is an inhibitor of digestive enzymes i.e., α-glucosidase and α-amylase enzymes, so it is suspected that acarbose cannot work effectively as an inhibitor of the rate of glucose diffusion (Hsiao et al., 2006). Another explanation is that the crude extract contains numerous metabolites, such as tannins, phenolics, saponins, etc., which might be capable of interacting with glucose, but acarbose as a single compound lacks this property. Research indicates that plant extracts can demonstrate glucose diffusion retardation indices (GDRI) ranging from 8 to 29%, with methanol extracts showing greater efficacy as inhibitors of glucose movement (Buthkar et al., 2018).

2.4. Protein analysis

The in-silico study started with the identification of the protein target, namely α-glucosidase. The crystal structure of α-glucosidase, known as 5ZCB, reveals the functional aspects of the protein target, indicating that it possesses residues situated within the permissible

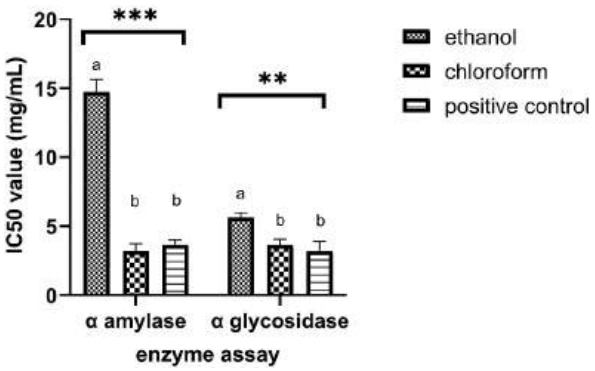

Fig. 1. The IC_{50} value of α-Amylase and α-Glucosidase enzymes inhibition activity of *Aquilaria malaccensis* Leaves Extracts. The data shown represent the average of triplicate assay. Significant differences between treatments for each assay are indicated as $^{**}p < 0.01$; $^{***}p < 0.0001$ using One Way ANOVA followed by Tukey post-hoc analysis.

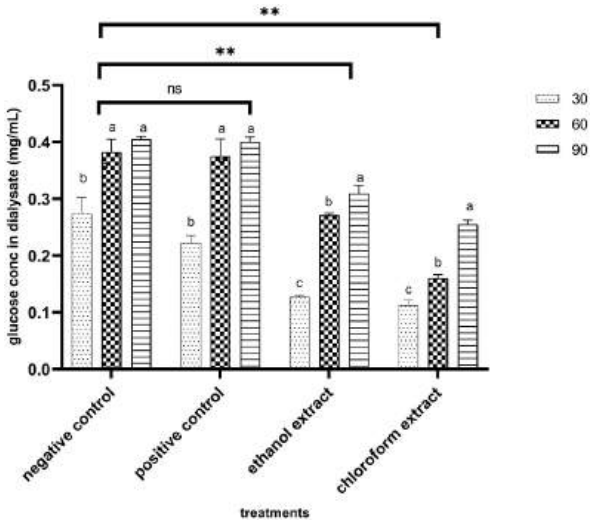

Fig. 2. Glucose diffusion inhibition capacity of ethanol and chloroform extracts of *Aquilaria malaccensis* leaves for 30, 60 and 90 min. Data represent the average of glucose concentration on the dialysate for three experiments. Significant differences between treatments are indicated as **p < 0.01 and ns for no significant different using One Way ANOVA. The letter above the bar represented the significance of different in sampling observation within a treatment, as determined by Tukey's post-hoc test.

region (Wibowo et al., 2019, 2020). Consequently, the secondary structures encompassing alpha helix, beta sheet, turn, and coils should inherently occupy their respective designated locations. Based on the results of the Ramachandran analysis of protein model 5ZCB, it is revealed that 99.6% of the amino acid residues are situated within the allowed regions, while 0.4% are found in the disallowed region (Fig. 3.). The specific residues found within the disallowed region are SER145 and LEU296.

The protein 5ZCB is comprised of 555 amino acids with a molecular weight of 64854.67 Da. It possesses a theoretical isoelectric point (pI) of 4.83, indicating its neutrality at this pH. The distribution of charged residues reveals 95 negatively charged residues (Aspartic acid and Glutamic acid) and 59 positively charged residues (Arginine and Lysine), contributing to its structural integrity and intermolecular interactions. Notably, the protein demonstrates stability with an instability index of 29.14, implying its resilience in biological environments. Furthermore, it displays a substantial hydrophobic character (aliphatic index: 72.16) and a slightly hydrophilic nature (GRAVY: −0.678), potentially influencing its folding, membrane interactions, and solubility in aqueous environments. From the analysis of the α-glucosidase protein, it is determined that 5ZCB can serve as a model for utilization in all subsequent in silico stages.

2.5. Toxicity analysis

The interesting result on the toxicity analysis (hepatoxicity, carcinogenicity, immunotoxicity, mutagenicity and cytotoxicity) was

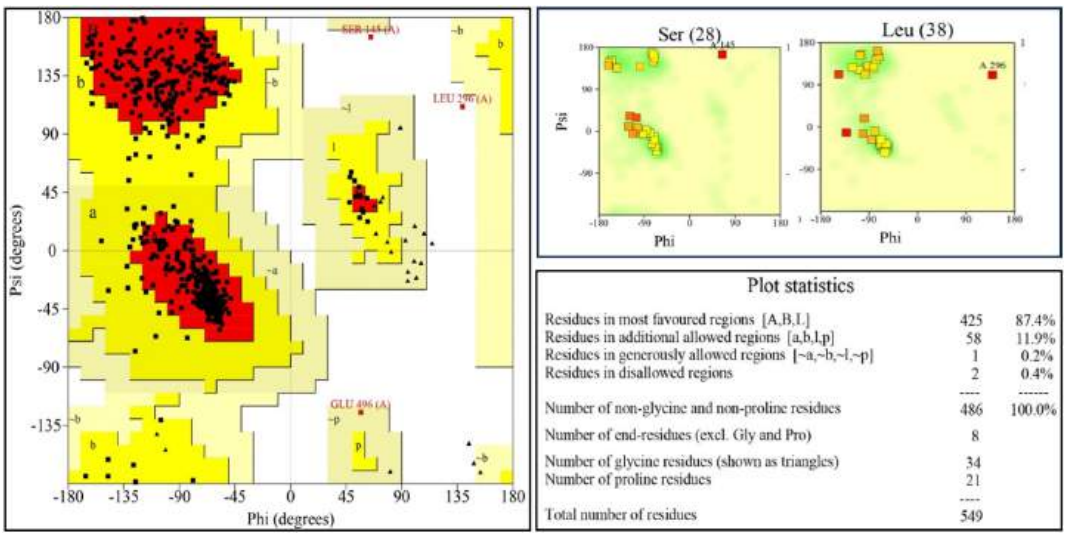

Fig. 3. Ramachandran plot of α-glucosidase 5ZCB

obtained for the among 10 secondary metabolites of *A. malaccensis*. One of these, calarene shows a possibility of being immunotoxic.

Hence, the analysis indicates that 11-Octadecenoic acid, decanoic acid, and 1-heptadecyne are secondary metabolite compounds with a relatively high level of oral toxicity, falling into class 2. The LD_{50} (Lethal dose, 50%) values for decanoic acid, 11-octadecenoic acid, and 1-heptadecyne are 48 mg/kg, 300 mg/kg, and 48 mg/kg, respectively. The obtained results, for the LD_{50} in silico analysis are reported in supporting information. Regarding the acarbose, this result indicated that it may exhibits hepatoxicity and immunotoxicity (Table 1.). The assessment of toxicity is crucial in the drug development process, ensuring that a compound exhibits therapeutic benefits while maintaining an acceptable safety profile.

2.6. In silico molecular docking

The objective of the in silico molecular docking investigation was to elucidate potential metabolites derived from chloroform extracts of *A. malaccensis* leaves, which could act as inhibitors of α-glucosidase enzyme activity. The results demonstrated that only 5-Hydroxy-4′,7-dimethoxyflavone and epifriedelanol exhibited superior binding affinities compared to acarbose, with values of −7.2 kcal/mol and −7.8 kcal/mol, respectively compared to acarbose with value of −7.0 kcal/mol (Fig. 4.). Powerful non-covalent interactions between molecules, such as hydrogen bonding, electrostatic interactions, and hydrophobic as well as van der Waals forces, define enhanced binding affinities (Djunaidi et al., 2023).

5-Hydroxy-4′,7-dimethoxyflavone is a flavonoid compound found in plants and has attracted scientific interest due to its unique structure with hydroxyl (-OH) groups at positions 5 and 7, and methoxy (-OCH_3) groups at positions 4′ and 7. Xie et al. (2019) discovered that when dimethoxyflavone was orally administered to diabetic rats induced with STZ (streptozotocin), it significantly reduced blood sugar levels and glycosylated hemoglobin. Additionally, the compound resulted in significant increases in C-peptide, insulin, hemoglobin, and total protein content ($p < 0.05$). Moreover, dimethoxyflavone exhibited antioxidant effects by elevating non-enzymic antioxidants in the system.

Furthermore, the administration of dimethoxyflavone demonstrated a hypolipidemic effect, effectively reducing serum triglyceride levels, total cholesterol, and low-density lipoproteins. The histopathological examination of rat pancreases revealed the preservation of β cell integrity in STZ-induced diabetic rats, indicating its potential protective effect on pancreatic cells. Meanwhile epifriedelanol is a triterpenoid compound found in various plant sources, including leaves, fruits, and barks. Triterpenoids are known for their diverse biological activities, encompassing antioxidant, anti-inflammatory, and potentially antidiabetic properties (Saha, et al., 2010). The binding sites (Fig. 5.) of acarbose with the α-glucosidase protein are situated at GLU(A)243, LYS(A)239, GLY(A)273, LYS(A)242, GLU (A)271, ASP(A)272, ASN(A)275, PHE(A)276, ALA(A)247, THR(A)253, PHE(A)246, ILE(A)251, TYR(A)249, MET(A)252, and ASN(A) 277. Meanwhile, 5-Hydroxy-4′,7-dimethoxyflavone is located at TRP(A)318, ASN(A)316, VAL(A)269, PHE(A)276, ASN(A)277, ALA (A)270, (LYS(A)242, THR(A)253, ILE(A)251, PHE(A)246, ALA(A)247, (TRP(A)6, GLU(A)271 and LYS(A)7. On the other hand, epifriedelanol is found at LEU(A)219, LYS(A)290, ASP(A)289, LEU(A)287, GLY(A)286, ASN(A)258, MET(A)229, PHE(A)225, TRP(A) 288, GLU(A)141, and PRO(A)223. Acarbose and 5-Hydroxy-4′,7-dimethoxyflavone share several common amino acids in their binding locations, including ASN(A)277, PHE(A)276, THR(A)253, PHE(A)246, and GLU(A)271.

Based on the results of this molecular docking study reported on Fig. 5, significant conclusions could draw regarding the potential of the metabolite compounds (Widyarti et al., 2023a,b) derived from *A. malaccensis*, particularly 5-Hydroxy-4′,7-dimethoxyflavone and epifriedelanol, as inhibitors of α-glucosidase. Epifriedelanol display distinct binding sites that do not overlap with acarbose, a known alpha glucosidase inhibitor already used for diabetes management. The non-overlapping binding sites indicate that epifriedelanol could function independently or complementarily alongside acarbose in inhibiting the α-glucosidase enzyme. This implies that these metabolite compounds might offer a supplementary or alternative therapeutic approach for patients who are already receiving acarbose treatment. The advantage of having different binding sites lies in the potential synergistic effect (Ludlow, et al., 2015). Meanwhile, in the case of 5-Hydroxy-4′,7-dimethoxyflavone, due to its shared binding locations with acarbose along with a lower binding energy, this compound has the potential to competitively replace acarbose. However, further molecular dynamics testing is necessary to confirm this. The combination of acarbose with metabolite compounds may exert a more potent inhibitory impact on the α-glucosidase enzyme, resulting in enhanced glucose control and improved management of diabetes. Molecular dynamic simulation is required to assess the stability of the alpha glucosidase protein when inhibited by the control acarbose and epifriedelanol.

Table 1
The results of the toxicity analysis of various secondary metabolite compounds from *A. malaccensis* and the control (Acarbose). The value that is next to active or inactive is the level of machine learning's confidence towards the decision; the closer it is to 1, the more confident it is towards the data's outcome.

	Metabolites	Hepatoxicity	Carcinogenicity	Immunotoxicity	Mutagenicity	Cytotoxicity
1	Acarbose	Active (0.65)	Inactive (0.84)	Active (0.99)	Inactive (0.76)	Inactive (0.70)
2	Palustrol	Inactive (0.76)	Inactive (0.71)	Inactive (0.80)	Inactive (0.73)	Inactive (0.90)
3	Calarene	Inactive (0.81)	Inactive (0.73)	Active (0.54)	Inactive (0.72)	Inactive (0.68)
4	9-Octadecen-1-ol	Inactive (0.89)	Inactive (0.92)	Inactive (0.91)	Inactive (0.96)	Inactive (0.82)
5	9-Hexadecenoic acid	Inactive (0.55)	Inactive (0.64)	Inactive (0.99)	Inactive (1.0)	Inactive (0.71)
6	Decanoic acid	Inactive (0.52)	Inactive (0.63)	Inactive (0.99)	Inactive (1.0)	Inactive (0.74)
7	3-Eicosyne	Inactive (0.73)	Inactive (0.57)	Inactive (0.98)	Inactive (0.99)	Inactive (0.78)
8	11-Octadecenoic acid	Inactive (0.55)	Inactive (0.64)	Inactive (0.99)	Inactive (1.0)	Inactive (0.71)
9	1-Heptadecyne	Inactive (0.76)	Inactive (0.55)	Inactive (0.96)	Inactive (0.99)	Inactive (0.77)
10	5-Hydroxy-4′,7-dimethoxyflavone	Inactive (0.71)	Active (0.53)	Inactive (0.95)	Inactive (0.54)	Inactive (0.67)
11	Epifriedelanol	Inactive (0.78)	Inactive (0.79)	Inactive (0.59)	Inactive (0.87)	Inactive (0.93)

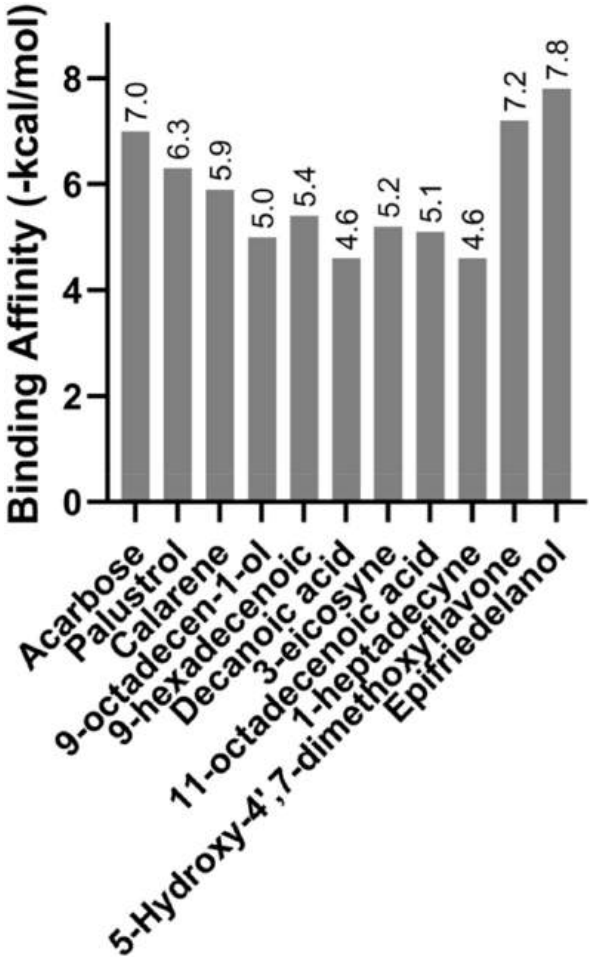

Fig. 4. Binding Affinity of Receptor (α-glucosidase) – Ligand (positive control and all compounds) (-kcal/mol).

2.7. Molecular dynamic simulation

Based on the findings from molecular dynamics simulations, it has been observed that there are no significant differences in the stability of the α-glucosidase protein complexed with 5-Hydroxy-4′,7-dimethoxyflavone and epifriedelanol, compared to the control, acarbose. The root means square deviation (RMSD) (Fig. 6.) of the protein backbone remains consistently below 2.2 nm throughout the simulations, with an RMSD value below 3 indicating the stability of the protein during the simulation (Wibowo et al., 2021). Furthermore, the total energy calculations for the complexes show values of −1650413.01 kJ/mol for the acarbose complex, −1652263.067 kJ/mol for 5-Hydroxy-4′,7-dimethoxyflavone, and −1651295.051 kJ/mol for epifriedelanol.

These results suggest that both 5-Hydroxy-4′,7-dimethoxyflavone and epifriedelanol form stable complexes with the α-glucosidase protein, akin to the control compound acarbose. The consistently low RMSD values indicate that the protein remains in a stable conformation during the simulations, implying that these ligands do not induce significant structural perturbations. The calculated total energies further support the stability of the complexes.

2.7.1. MD acarbose

In the acarbose-protein complex, hydrogen and hydrophobic bonds predominantly govern per-residue contacts, particularly involving amino acids 249 to 280. Notably, the per-residue contact graph exhibited a continuous line until the simulation's end, signifying the enduring binding of the ligand to the receptor. This observation finds further support in data concerning ligand movement, which demonstrates the persistent association of the ligand with the receptor throughout the simulation period, spanning from 0 ps to 15000 ps. Additionally, analysis of the radius of gyration data reveals that the protein's compactness remains unaffected upon acarbose binding, as indicated by minimal changes in peak values. Some fluctuations (Fig. 7.) are observed in a few amino acids, namely LYS(A)132, LEU(A)287, LYS(A)424, LYS(A)453, LYS(A)218, and TRP(A)288, with respective values of 3.156 Å, 3.252 Å, 3.43 Å, 3.433 Å, 3.733 Å, and 4.232 Å.

While a few amino acids may exhibit fluctuations that could be considered less stable, the majority of the protein-ligand complex in the molecular dynamic simulation remains relatively stable. The protein's overall compactness, as inferred from the radius of gyration

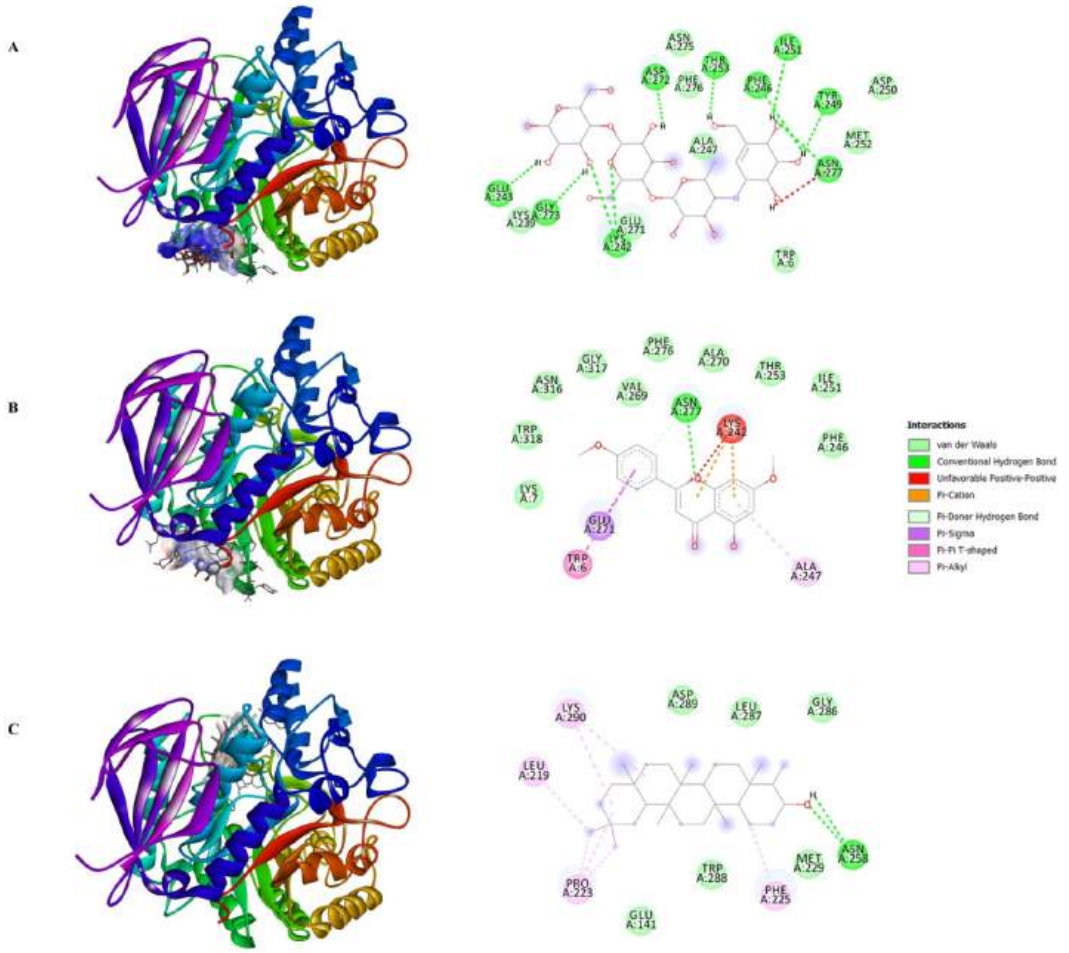

Fig. 5. Site binding analysis of α-glucosidase complex with (A) Acarbose, (B) 5-Hydroxy-4′,7-dimethoxyflavone, (C) Epifriedelanol.

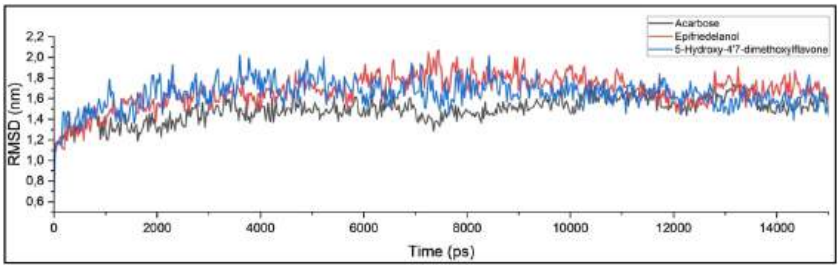

Fig. 6. RMSD backbone of α-glucosidase complexed with Acarbose (black line), Epifriedelanol (red line), and 5-Hydroxy-4′,7-dimethoxyflavone (blue line).

data, remains preserved with minimal changes in peak values, further supporting the complex's stability. Additionally, the persistent binding of acarbose to the receptor throughout the simulation, as observed in the per-residue contact graph and ligand movement analysis, strengthens the indication of the complex's overall stability.

2.7.2. Molecular dynamic 5-hydroxy-4′,7-dimethoxyflavone

In the 5-Hydroxy-4′,7-dimethoxyflavone-protein complex, hydrophobic interactions play a prominent role in influencing the per-residue contacts, particularly involving amino acids 249 to 280.

Additionally, hydrogen bonds are observed in amino acids 260, further contributing to the overall stability of the complex. This observation is corroborated by the data on ligand movement, which demonstrates the continuous association of the ligand with the receptor throughout the entire simulation duration (0 ps–15000 ps). Moreover, the binding of 5-Hydroxy-4′,7-dimethoxyflavone does

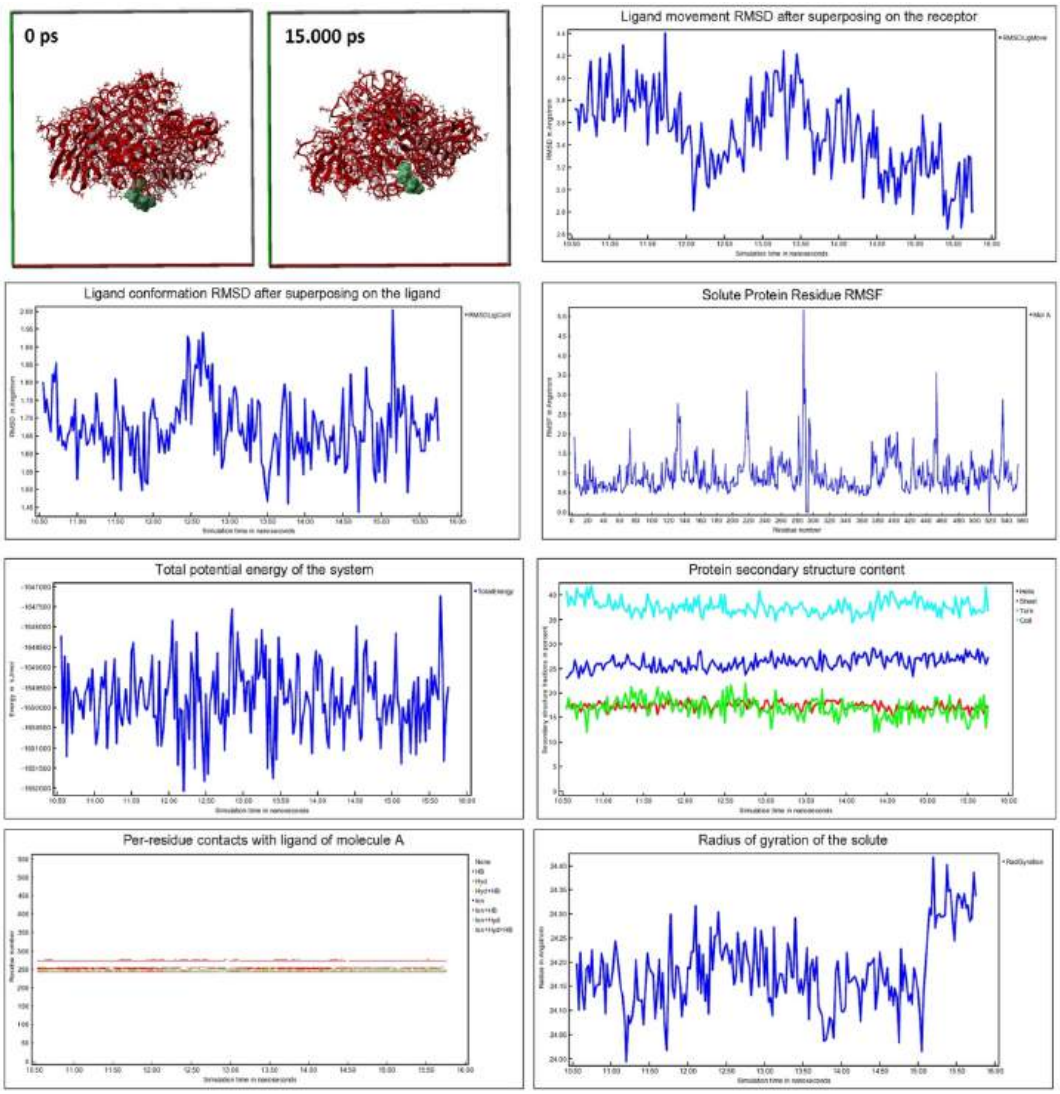

Fig. 7. Molecular dynamic simulation result of Acarbose + α-Glucosidase.

significantly impact the compactness of the protein, as reflected in the maximal changes observed in peak values from the radius of gyration data. Notably, in contrast to Acarbose, 5-Hydroxy-4′,7-dimethoxyflavone does not induce substantial fluctuations in all amino acids of the α-glucosidase. The fluctuations observed in specific amino acids, namely LYS(A)4 (2.453 Å), TRP(A)288 (2.474 Å), ASP(A) 272 (2.701 Å), LYS(A)218 (2.711 Å), LYS(A)453 (2.764 Å), and LYS(A)535 (2.855 Å), remain well within the established stability threshold of 3 Å (Fig. 8.). The change in ligand orientation can be explained based on the data obtained from ligand movement analysis, which indicates significant fluctuations. However, the compound still binds to the α-glucosidase protein.

2.7.3. Molecular dynamic epifriedelanol

In the complex of epifriedelanol with the protein, hydrophobic interactions are significant in influencing the contacts between specific amino acids, particularly those in the range of 220–290. This finding is supported by the ligand movement data, which shows the consistent association of the ligand with the receptor during the entire simulation period (0 ps–15000 ps). Furthermore, the binding of epifriedelanol to the protein does not significantly impact its compactness (Fig. 9.), as evidenced by the minimal changes observed in peak values derived from the radius of gyration data. Notably, in comparison to the control, epifriedelanol induces only slight fluctuations in all amino acids of the α-glucosidase. Specifically, the fluctuations observed in certain amino acids, namely LYS(A) 4 (2.826 Å), LYS(A)453 (2.836 Å), LEU(A)287 (2.877 Å), LYS(A)535 (2.974 Å), LYS(A)218 (3.356 Å), and LYS(A)424 (3.723 Å). The results of molecular dynamic trajectories were then further analyzed using PCA.

2.7.4. Principal Component Analysis of MD parameters

The PC1, PC2, and PC3 score axes in the score plot of the PCA analysis (Fig. 10) collectively account for more than 94.7% of the data

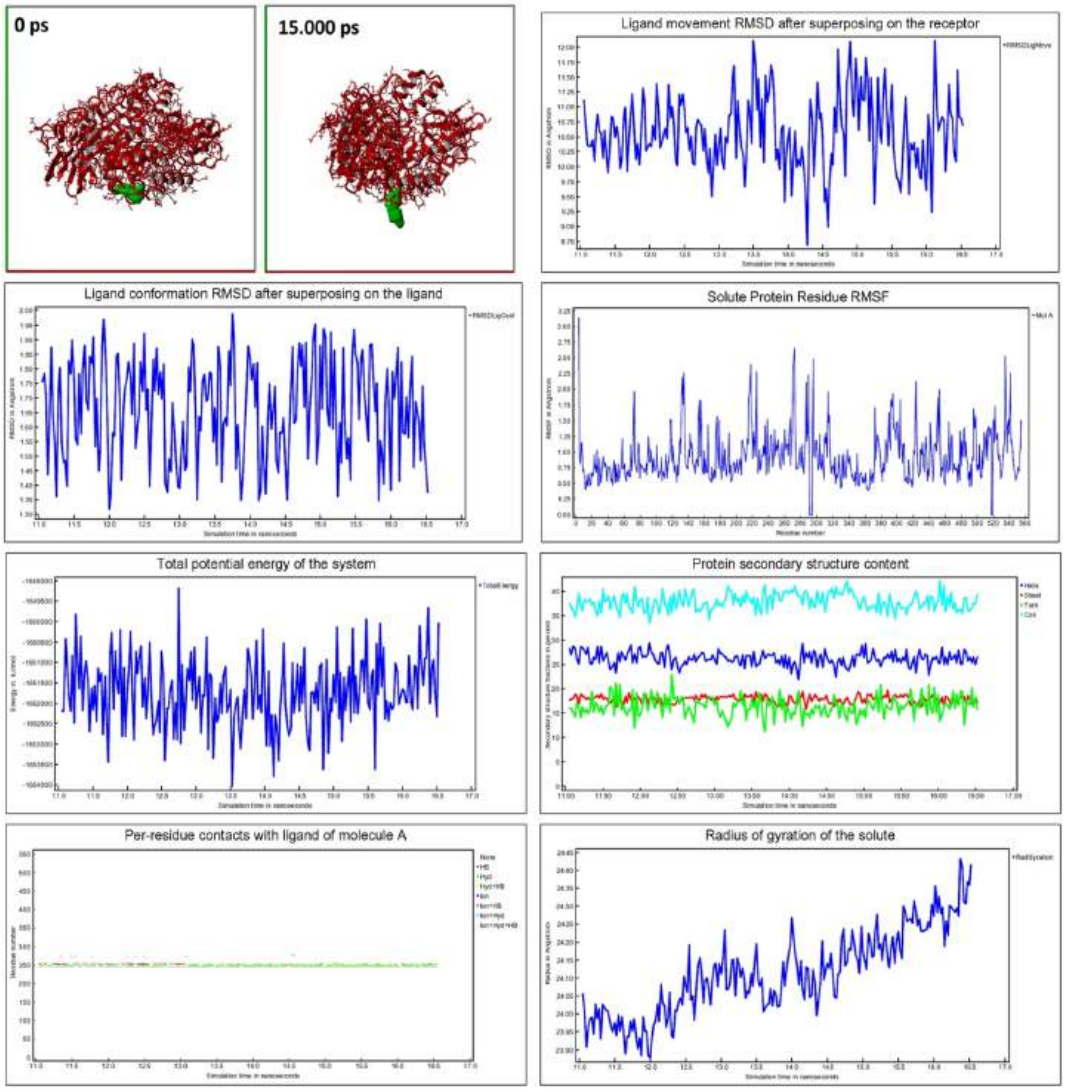

Fig. 8. Molecular dynamic simulation result of 5-Hydroxy-4′,7-dimethoxyflavone + α-Glucosidase.

variance from the diverse set of variables. This high percentage of variance explained indicates the reliability of the PCA results in comparing the outcomes of molecular dynamics (MD) simulations for both the Acarbose-protein and phytochemical-protein complexes. The PCA analysis reveals that all three complexes exhibit similar characteristics and overlapping traits in some aspects. This observation strengthens the findings from the molecular docking and dynamic analyses, which suggest that both epifriedelanol and 5-Hydroxy-4′,7-dimethoxyflavone can function as inhibitors similar to acarbose.

The distinguishing factor among the three complexes lies in the van der Waals (VdW) interactions. In summary, the comprehensive PCA analysis provides robust insights into the similarities and differences between the MD simulation outcomes of the Acarbose-protein and phytochemical-protein complexes. The findings highlight the potential inhibitory capabilities of epifriedelanol and 5-Hydroxy-4′,7-dimethoxyflavone, reinforcing their resemblance to acarbose. The distinct VdW interactions contribute to the variations observed among the three complexes. The scientific literature supports the significance of van der Waals forces in molecular dynamics. For example, research by Le et al. (2012) highlights the importance of these forces in governing various aspects of molecular interactions and behavior. Furthermore, studies by Dolenc et al. (2005) emphasize that van der Waals interactions are at least as important as hydrogen bonding in determining the stability of complexes formed between molecules. In conclusion, van der Waals forces play a central role in MD, exerting a profound influence on bond angles and distances, adsorption geometry, conformational stability, mechanical properties, and mass transport in diverse systems.

2.7.5. Density functional theory

Density functional theory (DFT) has emerged as a powerful and indispensable tool in modern quantum chemistry, enabling comprehensive investigations into molecular structures, thermodynamic properties, and electronic behaviors (Wibowo et al., 2021).

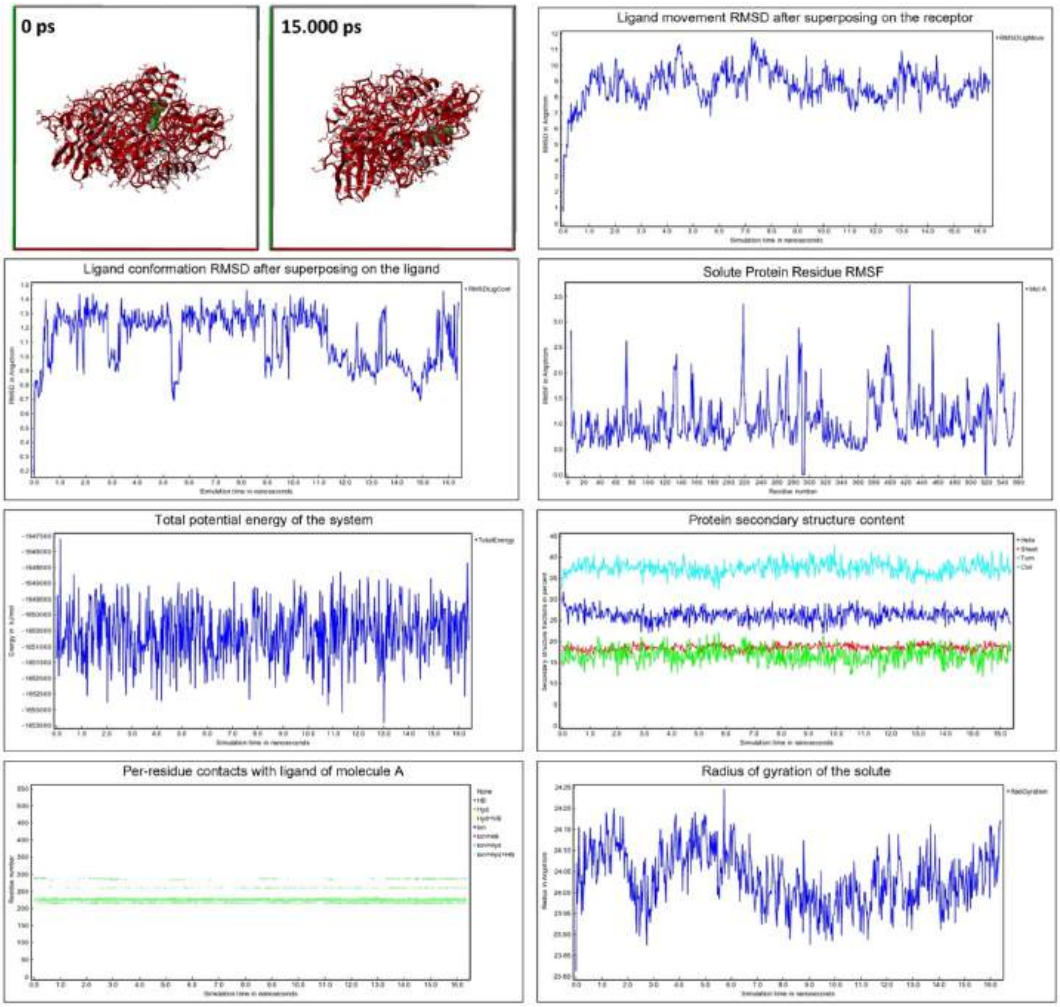

Fig. 9. Molecular dynamic simulation result of Epifriedelanol + α-Glucosidase.

In this study, we performed DFT calculations employing the B3LYP/6-31G(d,p) level of theory, utilizing Gaussian09 software to explore the molecular intricacies. Based on the analysis of total energy, Acarbose exhibits the lowest total energy value at −2387.27 Hartree, compared to 5-Hydroxy-4′,7-dimethoxyflavone (−1032.39 Hartree) and epifriedelanol (−1249.79 Hartree). Furthermore, concerning the dipole moments, the data reveals that epifriedelanol possesses the lowest value at 2.07 Debye, in contrast to acarbose (10.481 Debye) and 5-Hydroxy-4′,7-dimethoxyflavone (10.988 Debye). Moreover, the Electronic Spatial Extent (ESE) provides insights into the electron density's distribution in space. A larger ESE suggests a more delocalized or dispersed electron density over a larger volume, while a smaller ESE indicates a more localized or concentrated electron distribution. Notably, 5-Hydroxy-4′,7-dimethoxyflavone exhibits the lowest ESE value at 9639.09 au, whereas acarbose displays the highest value at 44494.67 au, followed by epifriedelanol at 16890.45 au.

A particular focus was directed towards the analysis of Frontier Molecular Orbitals (FMOs) (Fig. 11.), which hold paramount significance in understanding a molecule's fundamental characteristics. The Highest Occupied Molecular Orbital (HOMO) and Lowest Unoccupied Molecular Orbital (LUMO), known for their pivotal roles in shaping optical and electronic properties, elucidating quantum chemistry principles, and shedding light on biological mechanisms. The concept of the HOMO and LUMO holds significant importance in understanding a chemical species' electron-donating and electron-accepting capacities. Utilizing the (B3LYP)/6-31G(d,p) functional correlation within the DFT framework, we accurately determined the HOMO and LUMO for our molecular system. Remarkably depicted in the visualization of these orbitals (Fig. 11.) are distinctive regions colored in red and green, signifying their contrasting phases. The red regions denote heightened electron density, reflecting positive phases, while the green regions represent reduced electron density, corresponding to negative phases. This visually-rich depiction provides profound insights into the electron distribution within the molecular system, thereby offering valuable understanding of its electronic structure and reactivity.

The HOMO and LUMO energies serve as reliable indicators of a compound's electron-donating and electron-accepting capabilities. A lower LUMO energy implies a higher propensity for the molecule to accept electrons, whereas a higher HOMO energy suggests a greater likelihood of the molecule donating electrons. In our calculations, we found that among the compounds studied, 5-Hydroxy-

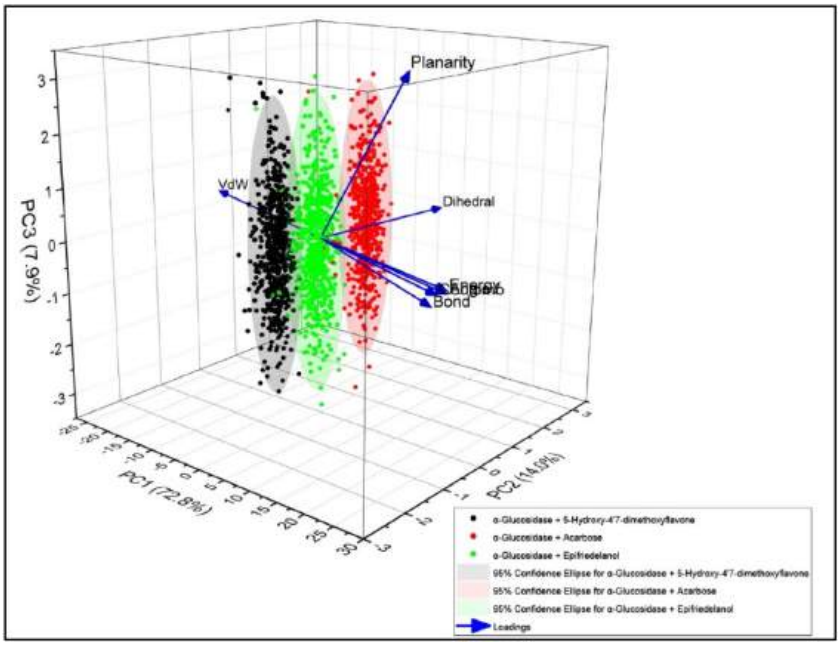

Fig. 10. Principal component analysis of MD Trajectories 0 ps–15000 ps.

4′,7-dimethoxyflavone exhibits the best electron-accepting capacity, while Acarbose demonstrates the most effective electron-donating behavior compared to both 5-Hydroxy-4′,7-dimethoxyflavone and epifriedelanol. Furthermore, the energy gap, a significant parameter governing chemical reactivity and structural stability, plays a crucial role. A smaller energy gap indicates a more facile transfer of electrons, ultimately bolstering the molecule's ability to neutralize free radicals and oxidative species, rendering it a potentially potent antioxidant. In this regard, 5-Hydroxy-4′,7-dimethoxyflavone possesses the smallest energy gap, followed by acarbose and epifriedelanol, respectively. The DFT results provide insights into the molecular dynamic simulation findings regarding the RMSF (Root Mean Square Fluctuation) of amino acid residues that have been inhibited by 5-Hydroxy-4′,7-dimethoxyflavone. As the most effective free radical scavenger compared to acarbose and epifriedelanol, the interactions between the compound and the catalytic site of the α-glucosidase enzyme are stabilized, resulting in RMSF values that do not exceed 3 Å for any amino acid residue in the system.

2.7.6. MEP (molecular electrostatic potential)

Molecular Electrostatic Potential (MEP) emerges as a critical parameter for evaluating the reactivity of an approaching electrophile towards a compound's active center, where electron distribution has the most pronounced effect. The analysis of MEP carries significant importance as it elucidates the molecular size, structure, and charge distribution, thereby offering valuable insights into the physico-chemical properties of the compound. This data enhances our understanding of molecular behavior and interactions, bolstering research into molecular structure-property relationships. Visual representation of electrostatic potential values through a diverse color range on the component map serves as a pivotal tool in comprehending the electronic characteristics of chemical compounds. A red hue signifies a negative electrostatic potential, indicating strong proton attraction to regions with high electron density. Conversely, a blue surface represents a positive electrostatic potential, denoting proton repulsion by atomic nuclei in regions with lower electron density and limited nuclear charge shielding. Green shades depict regions with neutral electrostatic potential. The study of MEP surfaces holds paramount significance in the realm of chemistry. Positive electrostatic potential regions act as favorable nucleophilic attack sites, promoting interactions with electron-rich species in chemical reactions. Conversely, negative electrostatic potential regions act as appealing electrophilic attack sites, encouraging interactions with electron-deficient species. A comprehensive analysis of the MEP surface provides invaluable insights into the compound's reactivity and its role in diverse chemical transformations (Garza et al., 2013).

As reported in Fig. 12., Acarbose displays multiple regions for electrophilic attack, followed by epifriedelanol, which features a major nucleophilic attack site at C29, H76, H75, H74, and H83, with the remaining areas being neutral. In contrast, in Acarbose, all oxygen atoms exhibit a red color, as acarbose has a higher number of oxygen atoms compared to 5-Hydroxy-4′,7-dimethoxyflavone and epifriedelanol, focusing on electrophilic attack in these regions. Furthermore, 5-Hydroxy-4′,7-dimethoxyflavone displays orange to red hues for all oxygen atoms, while carbon and hydrogen atoms exhibit variations in blue and green colors. The limitation of this study lies in the limited range of solvents employed for the extraction process. Further research incorporating a variety of solvents can provide additional comprehensive insights into the anti-diabetic potential of *A. malaccensis*. These findings hold promise for the development of novel antidiabetic agents and antioxidant therapies, paving the way for further research and exploration in the field of medicinal chemistry.

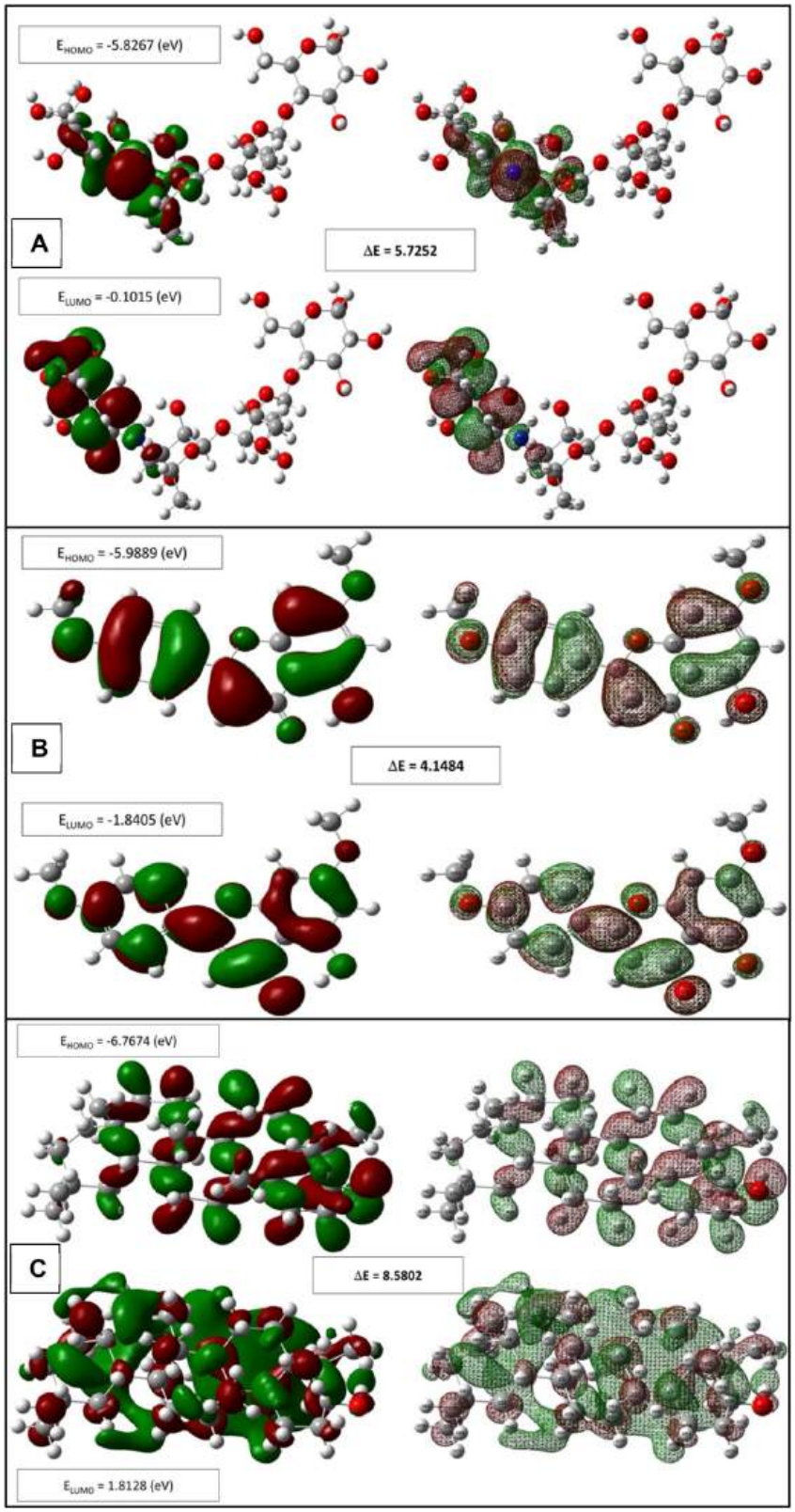

Fig. 11. Frontier molecular orbitals of (A) Acarbose (B) 5-Hydroxy-4′,7-dimethoxyflavone and (C) Epifriedelanol.

3. Conclusion

In conclusion, this study highlights the promising potential of *A. malaccensis* leaves and their metabolites as versatile contributors to both antidiabetic strategies and antioxidant interventions. Notably, the chloroform extract emerges as a compelling subject for further exploration in herbal medicine, displaying strong inhibition of α-amylase and glucose diffusion. Compounds such as 5-Hydroxy-4′,7-dimethoxyflavone and epifriedelanol exhibit noteworthy binding affinities to α-glucosidase, suggesting their efficacy as potent inhibitors for diabetes management. Molecular dynamics simulations and DFT calculations provided valuable insights into the stability and electronic properties of the α-glucosidase protein complexed with metabolite compounds from *A. malaccensis* leaves. This implies a complementary potential of these metabolites with Acarbose in inhibiting α-glucosidase, thereby enhancing glucose control and potentially improving diabetes management. Moreover, the analysis of molecular electrostatic potential surfaces emphasizes the potent free radical scavenging capabilities of 5-Hydroxy-4′,7-dimethoxyflavone, evident in a lower energy gap according to density functional theory analysis.

4. Experimental

4.1. Materials

Mature leaves of agarwood *A. malaccensis* were collected from Banyumas, Central Java, Indonesia. The plant species identification was conducted in the Plant Systematics Laboratory of Faculty of Biology, Universitas Gadjah Mada. The sample was cleaned in tap water and then air-dried overnight before the leaves were oven at 40 °C until reaching the constant weight. The samples were consistently weighed three times per week until reaching a stable state. After that, the leaves were pulverized using a blender and saved for the next experiment.

4.2. Plant extraction

About 10 g of the leaves powder was extracted using 150 mL of chloroform (Supelco, CAT. 102445) using the soxhlet apparatus for six cycles or until the solvent was clear. The heating power was adjusted to yield six extraction cycles within a span of 3 h, each lasting two cycles/hours. Then, the crude extract was evaporated using a rotary evaporator and stored at 4 °C for further use. A similar procedure was applied to the ethanol (Supelco, CAT. 100983) extracts (Calvaryni and Nuringtyas, 2022).

4.3. Assay of α-amylase inhibitory activity

A serial concentration of 2–10 mg/mL of chloroform and ethanol extracts was prepared for the enzyme assay. Acarbose (Sigma-Aldrich, St. Louis, MO, USA) was used as a positive control. The assay included four types of reactions, designated C0, C1, S0, and S1, to determine the % of inhibitory activity. C treatment was for control treatment in which samples were changed with buffer. C0 was the control without enzyme, while C1 was the control with enzyme. S was for sample treatment in which S0 was the sample without enzyme, and S1 was the sample with enzyme. The following procedure was done for the complete sample reaction with enzyme. In a glass tube, 0.5 mL of samples of each concentration were added with a similar volume of 1 U/mL α-amylase enzyme solution. The mixtures were incubated for 10 min at 37 °C; subsequently, 1% of starch substrate was added and re-incubated for 10 min. The reaction was terminated by adding 1 mL of DNS (3,5-Dinitrosalicylic acid) (Sigma-Aldrich, CAT. 128848) reagent and heating in a water bath at 100 °C for 5 min, then adding 10 mL of distilled water. The solution was then homogenized using a vortex, and its absorbance (Abs) was recorded using a UV–Vis spectrophotometer at 540 nm. For the blank, the sample was replaced with a phosphate buffer solution (pH 6.8) of the same volume and was subjected to the same processes as the sample. Data was presented in the form of % inhibition with the following formula (Lakshmanasenthil et al., 2018; Wickramaratne et al., 2016):

$$\%\ Inhibition = \frac{(C1 - C0) - (S1 - S0)Abs}{(S1 - S0)Abs}$$

The EC_{50} value was automatically determined using GraphPad Prism 5.01, employing the statistical model of Log (inhibitor) versus normalized response (variable slope) for data analysis.

4.4. Assay of α-glucosidase inhibitory activity

The α-glucosidase inhibitory assay was done with similar set of reactions to measure the inhibitory activity as per as α-glucosidase inhibitory assay (Lakshmanasenthil et al., 2018; Wickramaratne et al., 2016). A set of concentrations ranging from 2 to 10 mg/mL of chloroform and ethanol extracts was prepared. The positive control used acarbose at a similar serial concentration to the extracts. The blank solution used 2% of DMSO (Dimethyl sulfoxide) (Merck, CAT. 8418) to replace the sample. In a 96-well microplate, the solution with 120 μL of phosphate buffer pH 6.8 and 20 μL α-glucosidase enzyme (Sigma-Aldrich, CAT G8823) 0.5 U/mL were mixed. Subsequently, the mixtures were incubated at 37 °C for 15 min. After the incubation, 20 μL of 10 mM PNPG (4-Nitrophenyl-β-D-glucopyranoside) (Sigma-Aldrich, CAT N1627) substrate was added and incubated for 60 min at 37 °C. Then 80 μL of sodium carbonate 0.2 M was added to stop the reaction. The absorbance of the sample was measured using a microplate reader at a wavelength of 405 nm. Each extract was subjected to experimentation in triplicate. The data was provided as a % of inhibition, as specified in the α-glucosidase inhibitory assay.

4.5. Assay of glucose diffusion

The procedure for this experiment was done following the method developed by Qujeq and Babazadeh (2013). In the dialysis bag

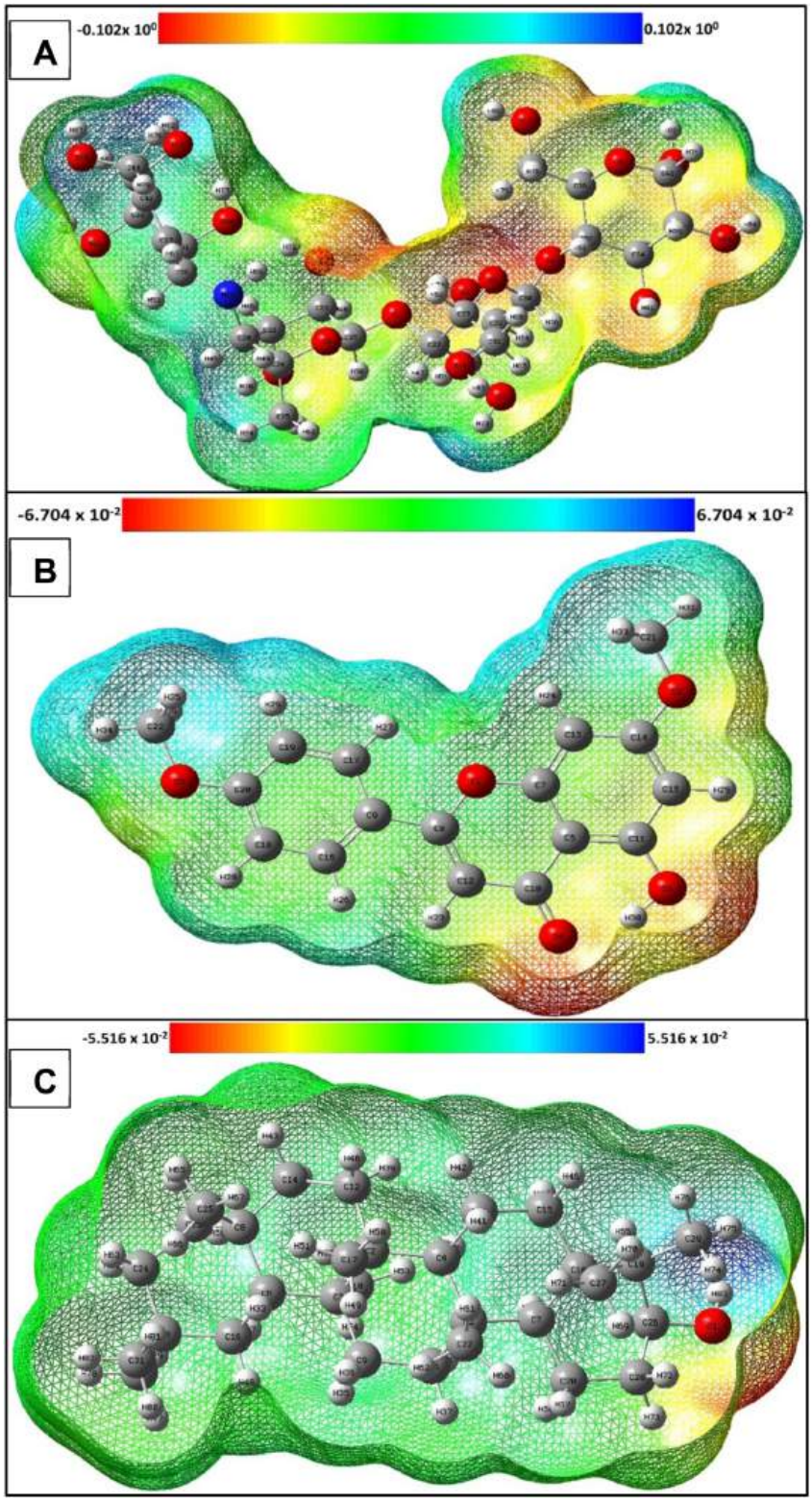

Fig. 12. MEP of (A) Acarbose (B) 5-Hydroxy-4′,7-dimethoxyflavone and (C) Epifriedelanol. Differences in color distribution signify diverse electrostatic characteristics (yellow: moderately electron-rich site, blue: electron-deficient site, light green: nearly neutral site, red: highly electron-rich site, white or grey: zero potential).

(MWCO 10 KDa, Sigma-Aldrich, St. Louis, MO, USA), a mixture of 6.25 mL of glucose solution (20 mM) and 1% of the sample was incubated in 50 mL of distilled water at 37 °C in an orbital shaker. The glucose content in the dialysate was determined every 30 min for 90 min. In the negative control, the sample was replaced with distilled water. Each extract was subjected to three repetitions of the experiment.

4.6. In silico study

In order to explore the potency of the *A. malaccensis* as antidiabetic, in silico study were conducted using secondary metabolites of *A. malaccensis* leaves obtained from Millaty et al. (2020) a nd Eissa (2022). The in silico analysis included toxicity analysis of the secondary metabolites of *A. malaccensis*, protein analysis on the target protein, molecular docking, molecular dynamics using PCA, and density functional theory analysis (Marzouk et al., 2022; Widyarti et al., 2023a,b; Djunaidi et al., 2023; Adli et al., 2024).

4.6.1. Toxicity analysis

Toxicity analysis was conducted using the open-source ProTox-II (https://tox-new.charite.de/protox_II/) accessed on April 18, 2023, where inputs in the form of canonical SMILES were analyzed based on oral toxicity, as well as other types of toxicity. Canonical SMILES were obtained from the PUBCHEM database with PUBCHEM ID access, namely Acarbose (41774), Palustrol (110745), Calarene (28481), 9-Octadecen-1-ol (8927), 9-Hexadecenoic acid (5181745), Decanoic acid (2969), 3-Eicosyne (549159), 11-Octadecenoic acid (5281127), 1-Heptadecyne (141274), 5-Hydroxy-4′,7-dimethoxyflavone (5281601), Epifriedelanol (119242).

4.6.2. Protein analysis

The protein used in this model was α-Glucosidase (PDB ID: 5zcb). Before proceeding to the protein docking stage, the protein was first analyzed for its quality using the Ramachandran Plot (PDBsum: http://www.ebi.ac.uk/thornton-srv/databases/pdbsum/) accessed on April 19, 2023. In this study, ProtParam, a computational tool widely used in molecular biology, was employed to analyze the physicochemical properties of protein sequences. Input sequences were accepted in both Fasta and ID formats, accompanied by SwissProt/TrEMBL accession numbers. The tool, integrated with SwissProt at web.expasy.org, facilitated the computation of key parameters, including molecular weight, amino acid composition, atomic composition, theoretical isoelectric point (pI), and instability index. Through these analyses, valuable insights into the unique characteristics of the proteins under investigation were gained.

4.6.3. Molecular docking

The protein target used in this study was the α-Glucosidase (PDB ID: 5zcb). This protein was obtained from the Protein Data Bank in pdb format. Protein target preparation was using the Discovery Studio 2016Client. The process carried out in this application was removing water molecules from protein and separating natural ligands from ligand-free proteins. The structure of the selected compounds in the extract served as ligand. Energy minimization of ligands was conducted in Open Bibel that integrated with PyRx 0.8. Docking calculations were performed using the Autodock Vina Wizard in the CBDOCK2 (https://cadd.labshare.cn/cb-dock2/php/index.php) accessed on April 20, 2023. The docking result of the selected CBDOCK2 was the first rank out of 10 docking modes. Docking validation had been performed by machine learning on the server. The docking results were visualized using the BIOVIA Discovery Studio 20.1.0 application to observe the binding interactions between the enzyme and the ligand (Wibowo et al. 2019, 2020).

4.6.4. Molecular dynamic (MD) simulation

YASARA was used to run MD simulations for 15,000 ps with physiological pH configurations at 7.4 and 0.9% NaCl for ion concentration as a mass fraction. The temperature used was 310K, and water was used as the solvent with a density of 0.997 g/l. The protein, ligand, water, and ion interactions in this study adhere to the AMBER14 force field. The simulation cell takes on a Cube shape. RMSD (root mean square deviation), RMSF (root mean square fluctuation), potential energy, protein secondary structure content, per-residue contacts with ligand, radius of gyration, and movie visualization were obtained from this MD simulation (Wibowo et al., 2022)

4.6.5. Principal Component Analysis of molecular dynamics

In this study, PCA was employed to comprehend the subtle differences among the structural and energy variables generated from MD simulations. PCA, a mathematical transformation tool utilized to reduce the dimensionality of large datasets for enhanced interpretability, played a pivotal role in the analysis. 15,000 ps of MD trajectory data were specifically considered for the PCA in this investigation, as this particular time frame demonstrated the greatest stability and equilibrium. The PCA analysis centered around crucial structural variables, including angle, dihedral, bond, van der Waals, Coulomb, VdW, total energy, and planarity energies. All components of the trajectory data used in PCA were normalized using OriginPro 2021. These variables were integral in elucidating any subtle changes in the protein structure following the addition of ligands. For the PCA analysis, Origin Pro 2021 in con junction with the PCA application v.1.50 package (Origin Lab, 2021) was employed, attesting to the advanced software used to conduct this comprehensive analysis.

4.6.6. Density functional theory analysis

The present investigation encompassed computational endeavors conducted utilizing the Gaussian 09 W computational suite, employing the density functional theory (DFT) methodology as harnessed within the aforementioned computational platform. Notably, the hybrid functional B3LYP, a merger of Becke's exchange and Lee, Yang, and Parr's correlation functionals (Wibowo et al., 2021), in conjunction with the 6-31G (d,p) basis set, was employed to undertake the quantum-chemical computations. Through Koopmans' theorem and molecular property computations, the investigation encompassed an examination of electronic properties, comprising the molecular electrostatic potential (MEP), dipole moment, and electronic spatial extent, along with crucial energy

descriptors such as the energy gap, E_{HOMO} (highest occupied molecular orbital energy), and E_{LUMO} (lowest unoccupied molecular orbital energy).

Author contributions

Conceptualization, S.W. (Syahputra Wibowo), S.K.W. (Sunia Kusuma Wardhani) and T.R.N (Tri Rini Nuringtyas); validation, S.W., T.R.N., L.H. (Lisna Hidayati), N.W. (Nastiti Wijayanti), J.C. (Jessica Costa), K.M. (Koichi Matsuo), Y.N. (Yudhi Nugraha), and J.E.S. (Josephine Elizabeth Siregar); investigation, S.W.; formal analysis, S.W., J.C., T.R.N., Y.N., amd J.E.S.; data curation, S.W.; writing—original draft preparation, S.W.; writing—review and editing, S.W. (Syahputra Wibowo), T.R.N; visualization, S.W.; supervision, T.R.N., K.M., J.C., Y.N., J.E.S. All authors have read and agreed to the published version of the manuscript.

CRediT authorship contribution statement

Syahputra Wibowo: Conceptualization, Data curation, Formal analysis, Investigation, Methodology, Project administration, Resources, Software, Validation, Visualization, Writing – original draft, Writing – review & editing. **Sunia Kusuma Wardhani:** Conceptualization. **Lisna Hidayati:** Supervision. **Nastiti Wijayanti:** Visualization. **Koichi Matsuo:** Supervision, Validation. **Jessica Costa:** Supervision, Validation. **Tri Rini Nuringtyas:** Conceptualization, Funding acquisition, Investigation.

Declaration of competing interest

The authors declare that they have no known competing financial interests or personal relationships that could have appeared to influence the work reported in this paper.

Data availability

Data will be made available on request.

Acknowledgement

This work was financially supported by Postdoctoral Program Universitas Gadjah Mada 2023 (contract number 1291/UN1/DITLIT/Dit-Lit/PT.01.02/2023) and Student lecturer Colaboration Grant 2019 of Faculty of Biology, Universitas Gadjah Mada. The authors declare no conflicts of interest in this research.

Appendix A. Supplementary data

Supplementary data to this article can be found online at https://doi.org/10.1016/j.bcab.2024.103152.

References

Adam, A.Z., Lee, S.Y., Mohamed, R., 2017. Pharmacological properties of agarwood tea derived from *Aquilaria* (Thymelaeaceae) leaves: an emerging Contemporary herbal Drink. J. Herb. Med. 10, 37–44. https://doi.org/10.1016/j.hermed.2017.06.002.

Adli, D.N., Sugiharto, S., Irawan, A., Tribudi, Y.A., Wibowo, S., Azmi, A.F.M., Sjofjan, O., Jayanegara, A., Tistiana, H., Wahyono, T., Aditya, S., Sholikin, M.M., Sadarman, S., 2024. The effects of herbal plant extract on the growth performance, blood parameters, nutrient digestibility and carcase quality of rabbits: a meta-analysis. Heliyon 10 (4), e25724. https://doi.org/10.1016/j.heliyon.2024.e25724.

Archer, M., Oderda, G., Richards, K., Turpin, S., 2013. Sulfonylurea Agents & Combination Products Drug Class Review. University of Utah College of Pharmacy [Final Report].

Brusotti, G., Cesari, I., Dentamaro, A., Caccialanza, G., Massolini, G., 2014. Isolation and characterization of bioactive compounds from plant resources: the role of analysis in the ethnopharmacological approach. J. Pharm. Biomed. Anal. 87, 218–228. https://doi.org/10.1016/j.jpba.2013.03.007.

Buthkar, M.A., Bhinge, S.D., Randive, D.S., Wadkar, G.H., Todkar, S.S., 2018. Screening of in-vitro hypoglycemic activity of *Murraya koenigii* and *Catharantus roseus*. Ars. Pharm 59 (3), 1–7. https://doi.org/10.30827/ars.v59i3.7413.

Calvaryni, N.M., Nuringtyas, T.R., 2022. Effects of fungicide treatment on metabolite profiles of *Aquilaria malaccensis*. Biocatal. Agric. Biotechnol. 43, 102407 https://doi.org/10.1016/j.bcab.2022.102407.

Chan, J.Y.W., Leung, P.C., Che, C.T., Fung, K.P., 2008. Protective effects of an herbal formulation of *Radix Astragali, Radix Codonopsis* and *Cortex Lycii* on streptozotocin-induced apoptosis in pancreatic β-cells: an implication for its treatment of diabetes mellitus. Phytother Res. 22 (2), 190–196. https://doi.org/10.1002/ptr.2285.

Djunaidi, I.H., Damayanti, C.A., Wibowo, S., Sjofjan, O., 2023. Exploring the potential of natural feed additives from herbs as an alternative to antibiotic growth promoters for Mojosari layer duck (*Anas javanica*) farming: in-silico and in-vivo studies. J. Indones. Trop. Anim. Agric. 48 (4), 243–257. https://doi.org/10.14710/jitaa.48.4.243-257.

Dolenc, J., Borstnik, U., Hodošček, M., Koller, J., Janežič, D., 2005. An ab initio QM/MM study of the conformational stability of complexes formed by netropsin and DNA. The importance of van der Waals interactions and hydrogen bonding. THEOCHEM 718, 77–85. https://doi.org/10.1016/J.THEOCHEM.2004.12.019.

Eissa, M.A., Hashim, Y.Z.H., Abdul Azziz, S.S.S., Salleh, H.M., Isa, M.L.M., Abd Warif, N.M., Abdullah, F., Ramadan, E., El-Kersh, D.M., 2022. Phytochemical Constituents of Aquilaria malaccensis leaf extract and their anti-inflammatory activity against LPS/IFN-γ-Stimulated RAW 264.7 cell line. ACS Omega 7 (18), 15637–15646. https://doi.org/10.1021/acsomega.2c00439.

Garza, A.J., Scuseria, G.E., Khan, S.B., Asiri, A.M., 2013. Assessment of long-range corrected functionals for the prediction of non-linear optical properties of organic materials. Chem. Phys. Lett. 575, 122–125. https://doi.org/10.1016/j.cplett.2013.04.081.

Hendra, H., Moeljopawiro, S., Nuringtyas, T.R., 2016. Antioxidant and Antibacterial activities of agarwood (*Aquilaria malaccensis* Lamk.) leaves. AIP Conf. Proc. https://doi.org/10.1063/1.4958565.

Herman, W.H., Kuo, S., 2021. 100 years of insulin: Why is insulin so expensive and what can be done to control its Cost? Endocrinol Metab Clin North Am 50 (3S), e21–e34. https://doi.org/10.1016/j.ecl.2021.09.001.

Hsiao, S.H., Liao, L.H., Cheng, P.N., Wu, T.J., 2006. Hepatotoxicity associated with acarbose therapy. Ann. Pharmacother. 40 (1), 151–154. https://doi.org/10.1345/aph.1G336.

Joo, H.J., Kang, M.J., Seo, T.J., Kim, H.A., Yoo, S.J., Lee, S.K., Lim, H.J., Kim, J.I., 2006. The hypoglycemic effect of *Saurus chinensis* Baill in Animal models of diabetes mellitus. Food Scie Biotech 15 (3), 413–417.

Lakshmanasenthil, S., Vinoth Kumar, T., Geetharamani, D., Shanthi Priya, S., 2018. α -amylase and α-glucosidase inhibitoryactivity of tetradecanoic acid (TDA) from sargassum wightii with relevance to type 2 diabetes mellitus. J. Biol. Act. Prod. Nat. 8 (3), 180–191. https://doi.org/10.1080/22311866.2018.1474803.

Le, D., Aminpour, M., Kiejna, A., Rahman, T., 2012. The role of van der Waals interaction in the tilted binding of amine molecules to the Au(111) surface. J. Phys.: Condens. 24 https://doi.org/10.1088/0953-8984/24/22/222001.

Ludlow, R., Verdonk, M., Saini, H., Tickle, I., Jhoti, H., 2015. Detection of secondary binding sites in proteins using fragment screening. Proc. Natl. Acad. Sci. U.S.A. 112, 15910–15915. https://doi.org/10.1073/pnas.1518946112.

Marzouk, H.A., Wibowo, S., Khotimah, H., Sumitro, S.B., 2022. Molecular interaction of centella asiaticabioactive compounds and Donepezil on alzheimer's protein through in silico studies. Research J.Pharma and Tech. 15 (11), 4887–4896. https://doi.org/10.52711/0974-360X.2022.00821.

Mat Rashid, Z., Mohd Nasir, N.N., Wan Ahmad, W.N., Mahmod, N.H., 2020. A-glucosidase inhibition, DPPH scavenging and chemical analysis of polysaccharide extracts of *Aquilaria* sp. leaves. J Agrobiotechnol 11 (2), 59–69. https://doi.org/10.37231/jab.2020.11.2.225.

McKinley, B.J., Santiago, M., Pak, C., Nguyen, N., Zhong, Q., 2022. Pneumatosis intestinalis induced by alpha-glucosidase inhibitors in patients with diabetes mellitus. J. Clin. Med. 11 (19), 5918. https://doi.org/10.3390/jcm11195918.

Millaty, I.N.K., Wijayanti, N., Hidayati, L., Nuringtyas, T.R., 2020. Identification of Anticancer compounds in leaves extracts of agarwood (*Aquilaria malaccensis* (Lamk.)). IOP Conf. Ser. Earth Environ. Sci. 457 https://doi.org/10.1088/1755-1315/457/1/012036.

Nabila, L., Ejaz, S., Madury, S.A., 2022. Drug-related problems (drps) in geriatric patients with type 2 diabetes mellitus (T2DM): a Review. IJPTher. https://doi.org/10.22146/ijpther.2695.

Nuringtyas, T.R., Isromarina, R., Septia, Y., Hidayati, L., Wijayanti, N., Moeljopawiro, S., 2018. The antioxidant and cytotoxic activities of the chloroform extract of agarwood (*Gyrinops versteegii* (Gilg.) Domke) leaves on Hela cell lines. AIP Con Proc. 2002 (1), 1–10. https://doi.org/10.1063/1.5050163.

Origin Pro, Version 2021. OriginLab Corporation, Northampton, MA, USA.

Poovitha, S., Parani, M., 2016. In vitro and in vivo α-amylase and α-glucosidase inhibiting activities of the protein extracts from two varieties of bitter gourd (momordica charantia L.). BMC Complement Altern Med 16. https://doi.org/10.1186/s12906-016-1085-1.

Qujeq, D., Babazadeh, A., 2013. The entrapment ability of aqueous and ethanolic extract of *Teucrium polium*: glucose diffusion into the external solution. Int J Mol and Cell Med 2 (2), 93–96. https://pubmed.ncbi.nlm.nih.gov/24551797.

Razak, R.N.H.A., Ismail, F., Isa, M.I., Wahab, A.Y., Muhammad, H., Ramli, R., Ismail, R.A.S., 2019. Ameliorative effect of *Aquilaria malaccensis* leaves aqueous extract on Reproductive toxicity induced by Cyclophosphamide in male rats. Malays. J. Med. Sci. 26 (1), 44–57. https://doi.org/10.21315/mjms2019.26.1.4.

Saha, P., Reddy, V., Konopleva, M., Andreeff, M., Chan, L., 2010. The triterpenoid 2-Cyano-3,12-dioxooleana-1,9-dien-28-oic-acid Methyl ester has potent antidiabetic effects in diet-induced diabetic Mice and Leprdb/db Mice. J. Biol. Chem. 285, 40581–40592. https://doi.org/10.1074/jbc.M110.176545.

Sudha, P., Zinjarde, S.S., Bhargava, S.Y., Kumar, A.R., 2011. Potent α-amylase inhibitory activity of Indian ayurvedic med plants. BMC Com Alt Med 11 (5), 1–10. https://doi.org/10.1186/1472-6882-11-5.

Telagari, M., Hullatti, K., 2015. In vitro α-amylase and α-glucosidase inhibitory activity of *Adiantum caudatum* Linn. And *Celosia argentea* Linn. Extracts and Fractions. Indian J. Pharmacol. 47 (4), 425–429. https://doi.org/10.4103/0253-7613.161270.

Tundis, R., Loizzo, M.R., Menichini, F., 2010. Natural Products as α-amylase and α-glucosidase inhibitors and their Hypoglycaemic potential in the treatment of diabetes: an Update. Mini-Rev. Med. Chem. 10 (4), 315–331. https://doi.org/10.2174/138955710791331007.

Venggadasamy, V., Ho, L., Ahmad, B., Kadir, K., 2021. Sexual Dysfunction in Asian Males with Type 2 Diabetes Mellitus. Progress In Microbes & Molecular Biology. https://doi.org/10.36877/pmmb.a0000259.

Wibowo, S., Sri, Widyarti, Akhmad, Sabarudin, Djoko, Wahono Soeatmadji, Sumitro, S.B., 2019. The role of astaxanthin compared withmetformin in preventing glycated human serum albumin from possible unfolding: a molecular dynamic study. Asian J. Pharmaceut. Clin. Res. 276–282 https://doi.org/10.22159/ajpcr.2019.v12i9.34617.

Wibowo, S., Sumitro, S.B., Widyarti, S., 2020. Computational Study of Cu2+, fe2+, fe3+, MN2+ and mn3+ binding sites identification on HSA 4K2C, IOP Conf. Ser. Mater. Sci. Eng. 833 (12052) https://doi.org/10.1088/1757-899x/833/1/012052.

Wibowo, S., Widyarti, S., Sabarudin, A., Soeatmadji, D.W., Sumitro, S.B., 2021. DFT and molecular dynamics studies of astaxanthin-metal ions (cu2+ and zn2+) complex to prevent glycated human serum albumin from possible unfolding. Helyon 7. https://doi.org/10.1016/j.heliyon.2021.e06548.

Wibowo, S., Costa, J., Baratto, M.C., Pogni, R., Widyarti, S., Sabarudin, A., Matsuo, K., Sumitro, S.B., 2022. Quantification and improvement of the dynamics of human serum albumin and glycated human serum albumin with Astaxanthin/Astaxanthin-metal ion complexes: physicochemical and computational approaches. Int. J. Mol. Sci. 23 (4771) https://doi.org/10.3390/ijms23094771.

Wickramaratne, M.N., Punchihewa, J.C., Wickramaratne, D.B.M., 2016. In-vitro alpha amylase inhibitory activity of the leaf extracts of Adenanthera pavonina. BMC Complement Altern Med 16, 1–5. https://doi.org/10.1186/s12906-016-1452-y.

Widyarti, S., Wibowo, S., Sabarudin, A., Abhirama, I., Sumitro, S.B., 2023a. Dysfunctional energy and future perspective of low dose H2O2 as protective agent in neurodegenerative disease. Helyon 9 (7). https://doi.org/10.1016/j.heliyon.2023.e18123.

Widyarti, S., Prakoso, B.D., Najihah, S., Wibowo, S., Fajar, Z.H., Permana, S., Sumitro, S.B., 2023b. Physicochemical characterization of astaxanthin-Cu complexes. Malays. J. Biochem. Mol. Biol. 26 (1), 83–89. https://msbmb2010.wixsite.com/mjbmb/december-2023.

Xie, Y., Zhang, Y., Su, X., 2019. Anti-diabetic and hypolipidemic effects of 5,7-dimethoxyflavone in streptozotocin-induced diabetic rats. Med Sci Monit 25, 9893–9901. https://doi.org/10.12659/MSM.918794.

Yeo, J., Young-Mi, K., Su-In, C., Myeong-Ho, J., 2011. Effects of a multi-herbal extract on type 2 diabetes. Chinese Med 6 (1), 1–10, 10.1186%2F1749-8546-6-10.